Particle Identification in CsI(Tl) Using Digital Pulse Shape Analysis

W.Skulski [a,1] and M.Momayezi [a]

[a] *X-Ray Instrumentation Associates, 8450 Central Av., Newark, CA 94560, USA*

Abstract

We developed particle identification (PID) in a CsI(Tl) crystal using digital pulse shape analysis. We present the details of the experiment, the data analysis, and the results. Two different methods of digital PID were applied to the same data set: the charge comparison method and the rise time inspection method. We have found the first method to be superior in most cases, consistent with the literature. The digital version of the charge comparison method compares favourably with its analog counterpart, achieving satisfactory proton/α–particle discrimination at energies as low as about 1 MeV, even though the measurements were carried out at the dynamic range of 40 MeV. This result clearly shows the power of digital electronics in achieving good particle identification for low amplitude signals.

1 Introduction

CsI(Tl) is widely used to achieve particle identification (PID), because in response to different ionizing radiation it emits "slow" and "fast" light components, whose amplitude ratio varies with the type of the radiation [1]. In nuclear physics CsI(Tl) has been used to build a number of 4π detector arrays with PID capability, such as the Dwarfball/DwarfWall [2], the MSU Miniball [3], the Microball [4], and others. These detector arrays have been used for nuclear reaction studies, as well as for in–beam selection of nuclear reaction channels with low cross sections. Their application was initially pursued for stable heavy ion beams, and recently also for radioactive beam accelerators. We have been motivated by such widespread use of the CsI(Tl) to develop PID algorithms using XIA's waveform digitizer and pulse processor DGF-4C [5].

[1] Corresponding author.

The PID algorithms using analog electronics can be broadly divided into three categories: the charge comparison, the zero–crossing method, and the ballistic deficit method (see [2–4,6–8] and references therein). The first method consits of integrating the light output from the CsI(Tl) in two different "time windows" separated by several μs, and calculating the ratio of the two results. Both of the latter methods rely on passing the input signal through two analog shapers with different time constants, and forming the PID index from their digitized outputs. All the above methods, which depend on a small number of data samples, are in principle less flexible than the digital filtering attainable with the digital pulse processor [5], which was developed for use in applications where high–resolution spectroscopy is to be combined with detailed pulse shape analysis of the detector signals.

The paper is organized as follows. The experimental setup is described, followed by details of data analysis. We present a digital implementation of two different methods to identify particles that have been detected by the CsI(Tl) crystal. Lower detection threshold and larger dynamic range are achieved in the present work, compared to results previously obtained using analog electronics. We conclude with a short summary and a discussion concerning application of digital electronics for achieving particle separation.

2 Experiment

The aim of the experiment was to derive the PID index from the shape of the signal from the CsI(Tl) crystal coupled to a photodiode, with emphasis on achieving good particle separation at a large dynamic range. A 1x1x1 cm^3 unpolished CsI(Tl) crystal was coupled with optical grease (Bicron 630) to a Hamamatsu photodiode type S3590-08 of 1x1 cm^2 active area. A piece of very thin aluminized mylar foil was placed in front of the crystal in order to improve light collection. The foil was sufficiently thin to cause a negligible energy loss of α–particles and protons entering the crystal. The crystal+diode assembly was wrapped with several layers of white Teflon tape to provide the best possible light collection. The quality of the combined photodiode/crystal assembly was assessed by measuring the energy resoluton for the 662 keV γ–ray from a ^{137}Cs source. We measured $FWHM = 12\%$, which is similar to the result reported by Moszynski *et al.* using analog electronics, namely $FWHM = 10.3\%$. We tentatively attribute our slightly worse energy resolution to imperfect light collection due to using an unpolished CsI(Tl) crystal. During the experiment the assembly was placed in a metal box to shield it from the ambient light, as well as from an electromagnetic interference. Radioactive sources were placed inside the box in close vicinity to the front face of the crystal. The experiment was conducted in air.

The photodiode was polarized with 70 V from a NIM high voltage supply, sufficient to cause total depletion of the diode. The diode was connected with a short BNC cable to a charge integrating preamplifier type 550 manufactured by eV Products. The preamplifier featured an RC reset feedback with an RC constant of 250 μs. The negative output pulses from the preamp were digitized at a rate of 40 MHz with 12 bit precision with the XIA DGF-4C digital spectrometer and wave form digitizer [5]. Only one out of four available DGF channels was used to collect data. The DGF-4C module was housed in a low noise CAMAC crate with an analog power supply. The crate was connected to a PC via a Jorway 73A SCSI crate controller. Standard DGF control software, the *DGF Viewer* developed at XIA, was used both to setup the module and to collect the data on a hard disk in list mode. The *DGF Viewer* runs under an interactive programming and data analysis environment IGOR [9], whose programming language and graphics were used to analyse the data offline.

Several radioactive sources were used during the experiment. Gamma sources included ^{241}Am, ^{137}Cs, and ^{60}Co. Alpha particles with energies up to about 4 MeV were emitted from a thick ^{241}Am source. Gamma rays and α–particles with energies up to about 5 MeV were emitted from a thick ^{nat}Th source, consisting of a 5x5mm^2 piece of a gas-flow lantern mantle [11]. A proton source was prepared by placing several layers of thin mylar foil in front of an 1μCi ^{241}Am open alpha source. The protons were elastically ejected from the mylar by α–particles, which were stopped in the mylar and did not enter the CsI(Tl) crystal. About two protons per minute with energies $0.5 > E > 2$ MeV were detected by the crystal.

3 Data analysis

For every event we recorded a time stamp (not used in this analysis), energy information, and a waveform with 1024 consecutive ADC samples, collected at 25 ns time intervals. Figure 1 shows several examples of such waveform data. The results reported in this paper were all obtained by processing the collected waveforms. The ADC traces were digitally filtered in order to reduce the high–frequency noise, whose presence is apparent in figure 1 in the form of little fluctuations. We found that smoothing the waveforms with a *boxcar algorithm* improved the rise time distributions, but it did not affect the PID. The boxcar algorithm consists of replacing the sample number n by an average of k samples before, k samples after, and the sample number n itself. Choosing $k = 2$ reduces the frequency bandwidth to roughly half its original value [10].

$$x'(n) = [x(n-k) + x(n-k+1) + \ldots + x(n+k)]/(2k+1) \qquad (1)$$

During the experiment, the trigger was placed at t_0 = 6 μs relative to the start of the ADC waveform, which covered a 25.6 μs time span (1024*25 ns = 25.6 μs). This allowed for enough ADC samples both before and after the trigger. The samples before the trigger are necessary in order to determine the "baseline level", relative to which all other measurements are performed. We used a 3.5μs averaging window positioned at the beginning of the waveform memory buffer, at a sufficient distance from t_0 to accomodate possible fluctuations of t_0, in order to measure the baseline value.

The energy values reported by the DGF on-board digital signal processor (DSP) were only used during setting up the experiment. During offline analysis the energy values were calculated by the host computer by averaging over parts of the ADC traces. The pulse height PH of each pulse was determined by averaging over ADC samples at the very end of the collected ADC trace, between t=20.5 and t=25.0 μs, i.e., 14.5 μs after the trigger instance t_0. Such a long delay after t_0 was motivated by the long time constant of the CsI(Tl) light output, of the order of 7 μs. The delay caused a sizeable decay of the collected charge (i.e., ballistic deficit), which can be corrected for by multiplying the measured PH by a constant factor. However, this correction was not done in this work. The gain of the analog DGF section was adjusted such that one ADC unit was very close to 10 keV, as determined by measuring the peak positions of the ^{60}Co γ–rays. We did not correct measured energy values for light output quenching in case of protons and α–particles. Based on the measured position of the ^{241}Am α–particle peak we estimate the effect of light quenching to be of the order of 20%.

Averaging consecutive ADC samples allows to measure the pulse height to a precision finer than the least significant bit (LSB) of the 12 bit digitizer. In fact, we determined the pulse height to about 1/8 of the LSB in this analysis (i.e., 32k channels). This allowed us to expand the dynamic range of the measurement without sacrificing the energy resolution. In this work the dynamic range was as large as 40 MeV (i.e., 4096 ADC steps times 10 keV). Such a range is appropriate for in-beam measurements with devices such as the Microball [4].

In addition to two main averaging windows (the baseline window and the pulse height window), a third one was used to implement the particle identification algorithm, as discussed in the next paragraph. Digital constant fraction timing was performed offline by calculating the time at which the waveform crossed a given fraction of the full pulse height relative to a baseline. The time interval elapsed between the 0.15 and 0.85 full amplitude crossings provided a measure of the signal rise time.

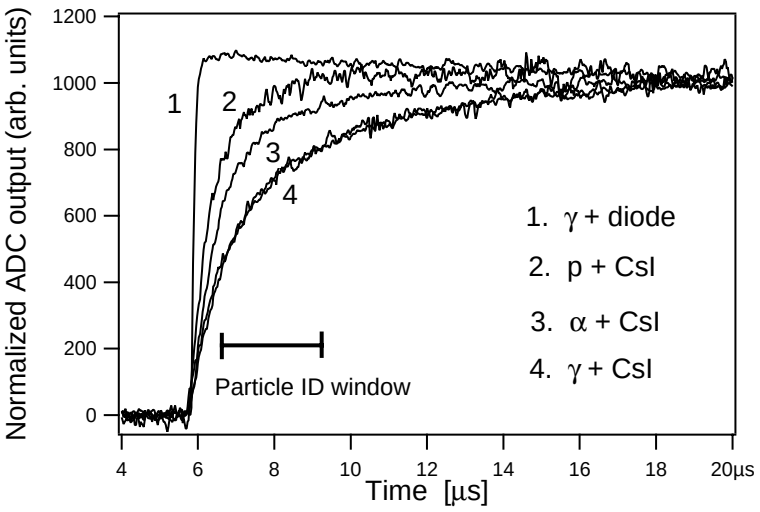

Fig. 1. Selected ADC waveforms show different pulse shape due to protons, α–particles, and γ–rays impinging on the CsI(Tl) crystal. In order to facilitate comparison the waveforms were normalized to the same height at t=20 μs, and their baselines were shifted to zero. Two traces due to α–particles are superimposed in order to demonstrate the constancy of the pulse shape for a given particle family. The trace number 1 was due to a photon conversion directly in the silicon photodiode. High frequency noise caused fluctuations clearly discernible in the data. The boxcar averaging was not applied to the traces in this figure.

4 Particle identification method and results

Figure 1 shows several ADC traces due to protons, α–particles, and γ–rays impinging on the CsI(Tl) crystal. Additionally we show an ADC trace due to a photon conversion directly in the silicon photodiode. This trace is set apart by its steep rise, as compared to all other traces. The particle identification index PID was computed as the ratio of the PID sum (shown in the figure) to the pulse height measured 14.5 μs after the trigger. It is obvious from the figure, that the best separation between particles detected in the CsI(Tl) crystal will be achieved by positioning the PID window where the separation between the traces is the largest, i.e., as shown in the figure. In principle, the PID values should span the range $0 < PID < 1$. The exponential decay of the preamplifier pulses can cause the PID to exceed 1.0 by about 10% for fast rising pulses, c.f. the trace number 1 in figure 1.

Both the position and the width of the PID window were optimized to provide the best separation between α–particles and γ–rays in the low energy range $E < 800$ keV, where obtaining good separation is the most difficult. The best α/γ separation was obtained with a relatively short PID window (duration between 2 and 2.5 μs), beginning 0.75 μs after the pulse start t_0, where t_0 was defined as the time at which the pulse exceeded 15% of its full amplitude.

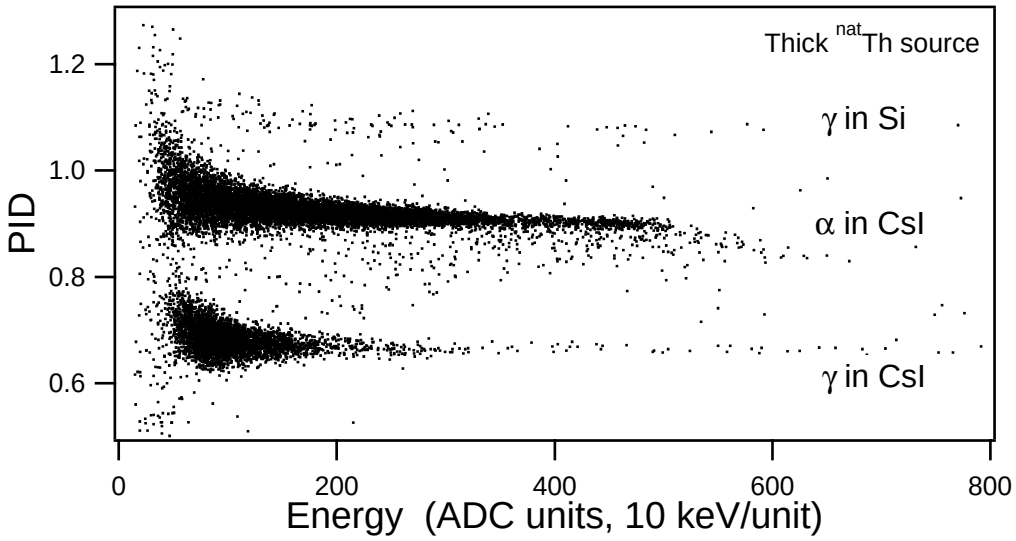

Fig. 2. Particle identification index PID plotted versus the measured energy of γ–rays and α–particles.

4.1 Alpha/gamma separation

Figure 2 shows the PID plotted as a function of the measured energy in the CsI(Tl) crystal. Three groups of events are clearly discernible: the events with $PID = 1.1$ are due to direct photodiode hits (such as the trace number 1 in figure 1), the events with $0.8 > PID > 1.1$ are due to α–particles, and events $0.6 > PID > 0.8$ are due to γ quanta. We have verified these assignments with radioactive sources that emit only one kind of radiation (^{60}Co and ^{137}Cs emit only γ–rays and ^{241}Am emit α–particles; the 60 keV ^{241}Am γ–ray fell below the detection threshold). The ridges corresponding to α–particles and γ–rays are very well defined and separated from each other down to the detection threshold. The PID distributions broaden as the energy approaches the threshold. There are also a few counts present between the ridges due to pileup events, that in principle can be identified and rejected by the DGF-4C firmware, or by the host computer based on the waveforms that differ from the waveforms of regular events. Pileup rejection was not performed in this work.

Figure 3 presents the PID index for two ranges of the measured energy, in order to show the excellent separation between different particle groups at energies as low as 1 MeV. The PID exhibits a weak energy dependence that shows up as a shift between the PID peaks for different energy ranges. The shift is so small that it is of no practical concern. The shift would be easy to correct with a small energy–dependent higher order correction applied during the offline analysis.

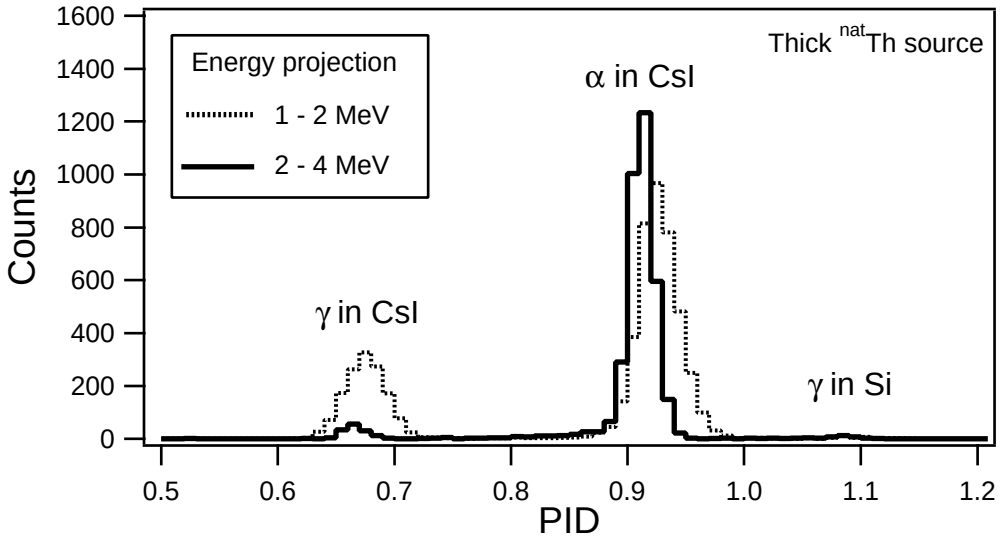

Fig. 3. The PID index for α–particles and γ–rays, projected from figure 2 for two energy ranges: 1 to 2 MeV (dashed line) and 2 to 4 MeV (solid line).

4.2 Proton/alpha/gamma separation

Separating protons from α–particles at low energies is difficult. Satisfactory separation was achieved down to $E_\alpha \approx 4$ MeV by Gal *et al.* using the ballistic deficit method [7] and analog signal processing. Even with their optimized processing scheme [8], separation could not be achieved at energies lower than $E_\alpha \approx 3$ MeV (*c.f.* figure 8 of ref. [8]). Achieving p/α separation at $E \approx 2$ MeV using analog signal processing was considered success by Moszynski *et al.* [6].

In this work we managed to achieve good p/α separation down to energies of $E \approx 1$ MeV, as shown in figure 4, where the PID distributions are compared for the α–particles emitted from the ^{nat}Th source and protons elastically ejected from the mylar foil. The p/α separation in figure 4 is almost as good as the separation achieved by Moszynski *et al.* at twice the energy range (our figure of merit M=0.8 versus their M=0.9, where M is defined [6] as the peak separation divided by the sum of peak FWHMs). We consider this result as very encouraging, especially given the fact that the noise in our detector was larger than the noise reported by Moszynski *et al.* for their setup.

We could not achieve good p/α separation below $E \approx 1$ MeV, because the proton ridge bended towards and eventually merged with the α–particle ridge at $E < 1$ MeV. Similar observation has been reported by Gal *et al.* [7], indicating that at low energies the dependence of the signal rise time on the proton energy will be a limiting factor for the low–energy threshold of the particle separation.

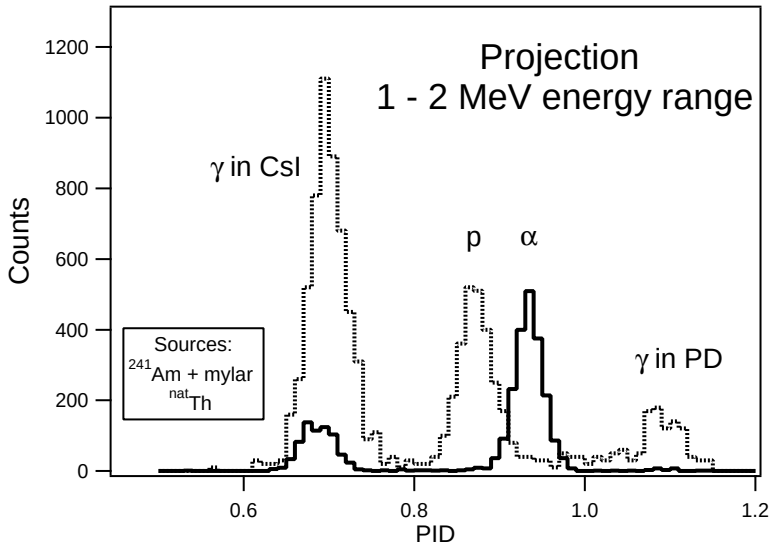

Fig. 4. The projection of the PID index in the energy range 1 to 2 MeV for protons elastically knocked out from the mylar foil (dashed line) and for the α–particles and γ–rays from the ^{nat}Th source (solid line). The γ peak observed in the case of proton source is due to natural background radiation.

4.3 PID obtained from pulse rise time

The inspection of pulse rise time is another commonly used method of particle discrimination in CsI(Tl) detectors, even though it is known to be not as good as the charge comparison method [4,6]. It is evident from figure 1 that pulses induced by different radiation species have different rise times, and therefore it was interesting to investigate the alternative method of obtaining PID from the pulse rise time. Points were located where the ADC waveforms cross the 15% and 85% levels of their full amplitude. The lower–level crossings were used as the trigger instances to anchor the PID window for the charge comparison method, as already discussed. The time differences between the lower–level and the upper–level crossings are plotted in figure 5.

Similar to figure 2, three groups of events are clearly discernible in figure 5. The events with the shortest rise time are due to γ conversion in the photodiode, consistent with figure 1. The events with the longest rise time are due to γ quanta detected in the CsI(Tl) crystal, and the events with intermediate rise times are due to α–particles detected in the crystal. The direct photodiode hits are clustered in a narrow strip close to $t = 0$. The separation between this group of events and all other events is much better defined than it was in the case of the charge comparison method. The separation is so good that it can be used to efficiently discriminate these events, as shown in figure 6, where the projected rise time distribution is plotted for all events from the figure 5. On the other hand, the separation between α–particles and γ–rays detected in the CsI(Tl) crystal is not as good as it is when using the charge comparison

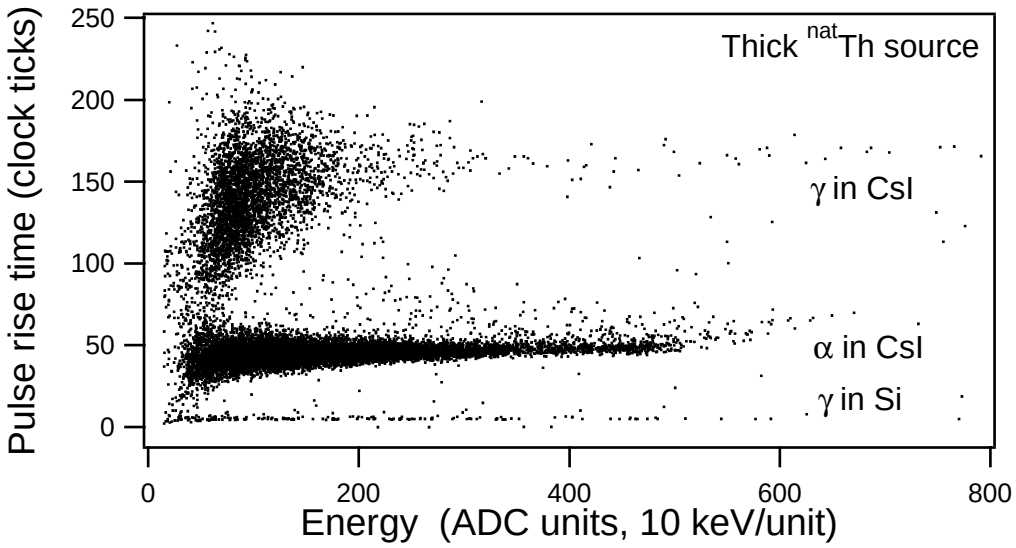

Fig. 5. Time difference between the 15% level crossing and the 85% level crossing, plotted as a function of energy. One clock tick equals 25 ns.

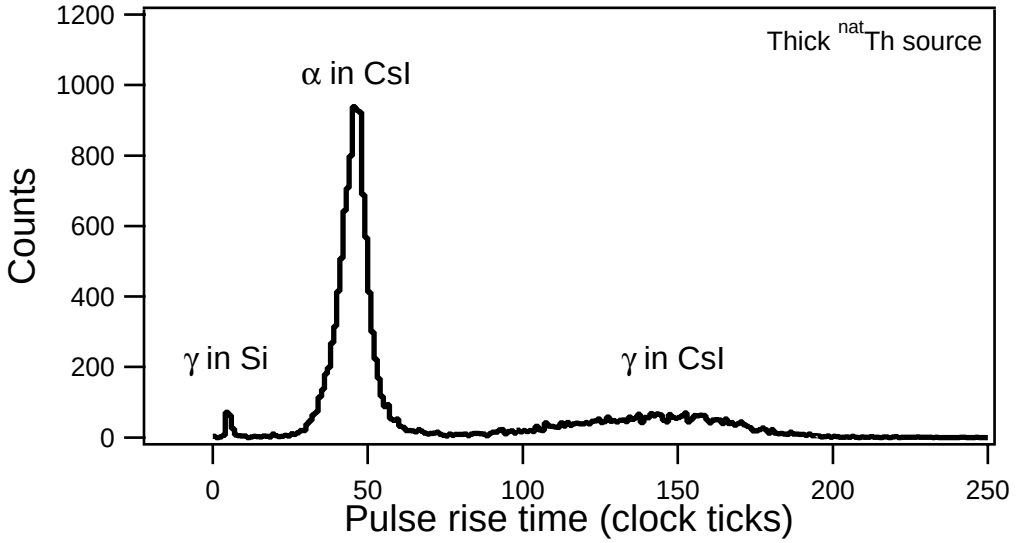

Fig. 6. The rise time distribution for all events of figure 5. One clock tick equals 25 ns.

method, consistent with the literature [6,4]. Nevertheless, it is clear that the rise time inspection of the digitally recorded waveforms can be used as an alternative PID method.

5 Summary and conclusions

We have developed particle discrimination using a CsI(Tl) crystal coupled to a photodiode, in conjuction with a digital analysis of recorded pulse shapes.

The performance of the digital method meets and exceeds the performance of classic methods using analog electronics. All the measurements were carried out with a dynamic range of 40 MeV, and with this large dynamic range good α/γ discrimination was achieved down to the detection threshold of about 0.5 MeV. The p/α discrimination was satisfactory down to energies as low as about 1 MeV. Two different methods of digital PID were applied to the same data set: the charge comparison method and the rise time inspection method. We have found the first method to be superior in most cases, consistent with literature. However, for some classes of events, such as direct photodiode hits, the rise time method works very well and allows to clearly separate these events from all the others. Present results clearly show the power of digital electronics in achieving good particle identification for low amplitude signals.

Acknowledgements

We wish to thank Jan Toke (University of Rochester) for loaning us the CsI(Tl) crystal used in this work. Discussions with P.Grudberg and W.K.Warburton are highly appreciated. J.Harris helped with setting up the preamplifier.

References

[1] G.Knoll *Radiation Detection and Measurement,* John Wiley and Sons, New York 1989.

[2] D.W.Stracener et al, *Dwarf Ball and Dwarf Wall: Design, instrumentation, and response characteristics...,* Nucl. Instr. and Meth. A294 (1990), 485.

[3] R.T.DeSouza et al, *The MSU Miniball 4pi fragment detection array,* Nucl. Instr. and Meth. A295 (1990) 109.

[4] D.G.Sarantites et al. *"The Microball": Design, instrumentation, and response characteristics...,* Nucl. Instr. and Meth. A381 (1996) 418.

[5] B.Hubbard-Nelson, M.Momayezi, W.K.Warburton, Nucl. Instr. and Meth. A422 (1999) 411.

[6] M.Moszynski et al. *Particle identification by digital charge comparison method applied to CsI(Tl) crystal coupled to photodiode,* Nucl. Instr. and Meth. A336 (1993), 587.

[7] J.Gal et al., *Particle discriminator for the identification of light charged particles with CsI(Tl) scintillator+PIN photodiode detector,* Nucl. Instr. and Meth. A366 (1995) 120.

[8] J.Gal et al., *Optimization of the particle discriminator based on the ballistic deficit method using delay–switched gated integrator,* Nucl. Instr. and Meth. A399 (1997) 407.

[9] IGOR programming environment and programming language, available from Wavemetrics Inc., www.wavemetrics.com.

[10] R.G.Lyons *Understanding Digital Signal Processing,* Addisson-Wesley, Reading MA 1997.

[11] E.I.Shabana et al., *Radioactivity in some gas-flow lantern mantles produced by different manufacturers,* Applied Radiation and Isotopes 51 (1999) 609.